© 2018. Published by The Company of Biologists Ltd | Development (2018) 145, dev159202. doi:10.1242/dev.159202

RESEARCH REPORT

Continuous root xylem formation and vascular acclimation to water deficit involves endodermal ABA signalling via miR165

Prashanth Ramachandran, Guodong Wang*, Frauke Augstein, Jan de Vries‡ and Annelie Carlsbecker§

ABSTRACT

The plant root xylem comprises a specialized tissue for water distribution to the shoot. Despite its importance, its potential morphological plasticity in response to environmental conditions such as limited water availability has not been thoroughly studied. Here, we identify a role for the phytohormone abscisic acid (ABA) for proper xylem development and describe how ABA signalling-mediated effects on core developmental regulators are employed to alter xylem morphology under limited water availability in *Arabidopsis*. Plants with impaired ABA biosynthesis and reduced ABA signalling in the cell layer surrounding the vasculature displayed defects in xylem continuity, suggesting that non-cell autonomous ABA signalling is required for proper xylem development. Conversely, upon external ABA application or under limited water availability, extra xylem strands were formed. The observed xylem developmental alterations were dependent on adequate endodermal ABA signalling, which activated *MIR165A*. This resulted in increased miR165 levels that repress class III HD-ZIP transcription factors in the stele. We conclude that a pathway known to control core developmental features is employed as a means of modifying plant xylem morphology under conditions of environmental stress.

KEY WORDS: ABA, *Arabidopsis thaliana*, HD-ZIP III transcription factors, miR165, Xylem

INTRODUCTION

Roots are responsible for water uptake and transport through their xylem strands. Although well-known responses to water-limiting conditions include a rapid induction of abscisic acid (ABA) levels (Xiong and Zhu, 2003), stomata closure and growth adjustments (Osakabe et al., 2014), little is known about how the water transporting tissue itself is affected. Understanding how and by what mechanisms xylem development adjusts to water deficit raises the possibility of developing crop-breeding strategies to produce varieties that are better able to tolerate limited water availability.

In primary development, the xylem tracheary elements form as thin protoxylem strands with annular or spiral secondary cell walls (SCWs) or as wider metaxylem with reticulated or pitted SCWs. In the root of *Arabidopsis thaliana*, xylem identity is determined by transcription factors (TFs) of the class III homeodomain leucine zipper (HD-ZIP III) family (Carlsbecker et al., 2010). The HD-ZIP III gene family encompasses *PHABULOSA* (*PHB*), *PHAVOLUTA* (*PHV*), *REVOLUTA* (*REV*), *Arabidopsis thaliana HOMEOBOX GENE 8* (*ATHB8*) and *CORONA* (*CNA*/*ATHB15*), which are post-transcriptionally controlled by microRNA165 (miR165) and miR166 (Reinhart et al., 2002; Rhoades et al., 2002). Genes encoding these miRNAs are transcriptionally activated in the endodermis, which surrounds the vasculature. miR165/166 then moves into the vasculature to restrict HD-ZIP III levels (Carlsbecker et al., 2010; Miyashima et al., 2011). This leads to lower peripheral HD-ZIP III levels, resulting in protoxylem formation, and higher central levels, resulting in metaxylem formation. Thus, the wild-type xylem axis develops two protoxylem strands flanking three central metaxylem strands (Fig. 1A), a pattern that is sensitive to miR165/166 level changes (Carlsbecker et al., 2010; Miyashima et al., 2011; Müller et al., 2016). Interestingly, miR165/166 levels are affected by abiotic stresses in a wide range of species (Eldem et al., 2012; Giusti et al., 2017; Kantar et al., 2010), suggesting that ABA-induced conditions confer developmental changes via miR165/166. Here, we address the role of ABA in *Arabidopsis* root xylem formation and in its crosstalk with miR165-HD-ZIP III developmental regulation, and the effects of water limitation on xylem morphology.

RESULTS AND DISCUSSION

ABA is required for proper root xylem development

To examine the potential importance of ABA for root xylem development, we analysed ABA deficient and signalling mutants (Fig. 1). *ABA2* and *ABA3* encode proteins involved in the final two steps in ABA biosynthesis, and *aba2-1* and *aba3-1* therefore have substantially reduced basal ABA levels (Léon-Kloosterziel et al., 1996). Tracing the protoxylem and metaxylem strands of primary roots of 5-day-old *aba2-1* and *aba3-1* mutants revealed that 40-60% of roots analysed displayed discontinuous or absent xylem strands, primarily metaxylem (Fig. 1B,C and Figs S1,S2). No other apparent anatomical differences were detected, apart from the quiescent centre (QC) divisions previously described by Zhang et al. (2010), and both mutants had significantly shorter roots than wild type (Fig. S2C). Treatment for 72 h with 5 nM ABA was sufficient to restore the xylem defects of *aba2-1* (Fig. 1B,C), whereas higher concentrations resulted in extra protoxylem strands next to the ordinary and seen as double protoxylem (Fig. 1C; see also below). Furthermore, wild-type plants treated for 72 h with the ABA biosynthesis inhibitor fluridone (Flu, 1 µM; Bartels and Watson, 1978) displayed discontinuous xylem (Fig. 1D,E), phenocopying ABA-biosynthesis mutants. Supplementing with 250 nM ABA alleviated these effects (Fig. 1E). Similarly, *abi1-1*, which carries a gain-of-function mutation in the ABI1 PP2C co-receptor phosphatase that renders the plant partially ABA insensitive (Leung et al., 1994;

Department of Organismal Biology, Physiological Botany, Evolutionary Biology Centre and Linnean Centre for Plant Biology, Uppsala University, Ullsv. 24E, SE-75651 Uppsala, Sweden.
*Present address: Key Laboratory of Ministry of Education for Medicinal Plant Resource and Natural Pharmaceutical Chemistry, National Engineering Laboratory for Resource Developing of Endangered Chinese Crude Drugs in Northwest of China, College of Life Sciences, Shaanxi Normal University, Xi'an, China.
‡Present address: Department of Biochemistry and Molecular Biology, Dalhousie University, Halifax, NS, Canada.

§Author for correspondence (annelie.carlsbecker@ebc.uu.se)

P.R., 0000-0001-8447-1691; G.W., 0000-0001-7440-0929; F.A., 0000-0003-3625-9703; J.d.V., 0000-0003-3507-5195; A.C., 0000-0002-8450-3718

Received 8 September 2017; Accepted 9 January 2018

Development (2018) 145, dev159202. doi:10.1242/dev.159202

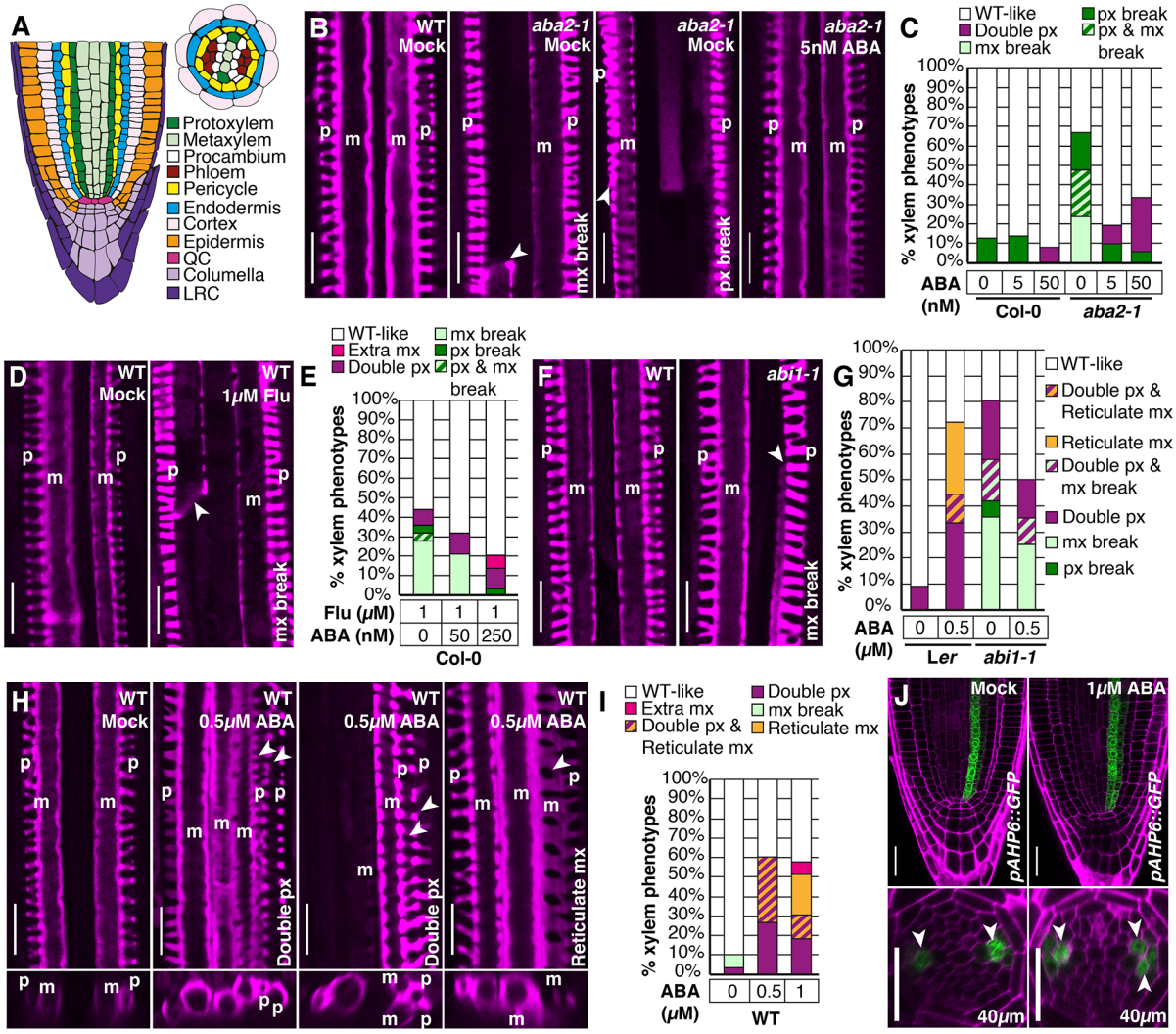

Fig. 1. ABA levels affect root vascular patterning in the meristem. (A) Schematic longitudinal and transverse sections of the *Arabidopsis* root meristem. Tissues are colour coded. (B) Confocal images of basic fuchsin-stained roots of wild type, *aba2-1* and *aba2-1* grown on 5 nM ABA. White arrowheads indicate xylem strand breaks. (C) Quantification of xylem phenotypes in wild type and *aba2-1* grown on 5 nM (wild type, *n*=22; *aba2-1*, *n*=21) and 50 nM ABA (wild type, *n*=13; *aba2-1*, *n*=18) for 72 h compared with mock (wild type, *n*=16; *aba2-1*, *n*=21). (D) Basic fuchsin-stained wild type treated for 72 h with 1 µM Flu. (E) Effects of 72 h co-treatment of Flu with 0 nM ABA (*n*=25), 50 nM ABA (*n*=29) and 250 nM ABA (*n*=29). (F) Xylem phenotypes of *abi1-1*. (G) Quantification of xylem phenotypes of wild type (L*er*) and *abi1-1*, grown on 0.5 µM ABA (wild type, *n*=19; *abi1-1*, *n*=25) compared with mock (wild type, *n*=12; *abi1-1*, *n*=24). (H) Xylem defects in wild type after 72 h 0.5 µM ABA treatment. Top: longitudinal optical sections; white arrowheads indicate defects. Bottom: transverse sections of the xylem axis. (I) Quantification of xylem phenotypes following 72 h on 0 (*n*=30), 0.5 (*n*=15) and 1 µM ABA (*n*=33). (J) *pAHP6::GFP* after 12 h of 0.5 µM ABA (*n*=19) or mock treatment (*n*=12). Radial images are 40 µm shootwards of QC. White arrowheads indicate protoxylem precursor cells. Number of independent experiments performed: C, 3; E, 2; G, 2; I, 3. p, protoxylem; m, metaxylem. Scale bars: 10 µm in B,D,F,H; 25 µm in J.

Meyer et al., 1994), displayed discontinuous metaxylem in both Col-0 and L*er* backgrounds (Fig. 1F,G, Fig. S2D,E). Neither in mutants nor upon Flu application is it likely that ABA levels or signalling are completely suppressed, possibly explaining the partial penetrance of the xylem phenotype; it is further likely that non-related pathways act redundantly with ABA to ensure xylem continuity. Nonetheless, our results suggest that ABA synthesis and signalling are crucial for proper root xylem development.

Elevated ABA levels induce extra xylem strands

To test the effects of elevated ABA levels, we treated 2-day-old wild-type seedlings for 72 h with varying concentrations of ABA. Root growth was compromised by ABA concentrations of 1 µM and above, as previously reported (Ghassemian et al., 2000), but was not affected by 0.5 µM ABA (Fig. S3A). In 60% of the roots, 0.5 µM ABA caused double protoxylem: the extra strand forming either aligned with or at an angle to the xylem axis (Fig. 1H,I, Fig. S1D). Furthermore, metaxylem SCWs became reticulate as opposed to pitted (Fig. 1H, Fig. S1D), and extra metaxylem appeared next to the xylem axis or prematurely in central positions (Fig. 1H, Fig. S1D). Higher ABA concentrations produced similar results (Fig. 1I). The *abi1-1* mutation prevented double protoxylem and reticulate metaxylem formation beyond what was already present in this mutant (Fisher's exact test, $P<0.05$) (Fig. 1G), suggesting that the ABA-induced xylem morphology changes were mediated via canonical ABA signalling, as defined by Cutler et al. (2010).

To determine whether the observed xylem morphology changes were the result of cell fate changes, we analysed the effect of ABA on the *pARABIDOPSIS HISTIDINE PHOSPHOTRANSFER PROTEIN6::GFP* (*pAHP6::GFP*) reporter, which normally

Development (2018) 145, dev159202. doi:10.1242/dev.159202

marks protoxylem plus neighbouring pericycle cell files within the meristem (Mähönen et al., 2006), and *pTARGET OF MONOPTEROS5::n3GFP*, which marks the immature xylem axis (De Rybel et al., 2013). Following 24 h of 0.5 µM ABA treatment, xylem changes were visible in 60% of 4-day-old plants (Fig. S3B), and already after 12 h treatment we detected *pAHP6::GFP* in double protoxylem cell files in 9/19 (47%) roots (Fig. 1J). Similarly, a 48 h ABA treatment increased the number of *pTMO5::n3GFP*-expressing cells to six (*n*=13/24, 54%), as opposed to five in mock-treated plants (*n*=18/21, 85%) (Fig. S3C). In addition, expression of the protoxylem-differentiation marker *pVASCULAR NAC DOMAIN7::YFP* (Kubo et al., 2005) expanded upon short-term high-concentration ABA treatment (Fig. S3D). These results suggest that ABA affects xylem cell fate.

Endodermal ABA signalling affects xylem patterning non-cell autonomously

ABA is predominantly localized to the endodermis (Ondzighi-Assoume et al., 2016). To determine whether ABA locally or non-cell autonomously influences xylem cell fate, we used *UAS::abi1-1* (Duan et al., 2013), crossed with GAL4 enhancer-trap lines, to reduce ABA signalling tissue specifically (Fig. 2A-E and Fig. S4). Assessing the xylem-pole pericycle *J0121≫abi1-1*, and the columella and lateral-root cap specific *J3411≫abi1-1* transactivation lines revealed that neither affected xylem morphology (Fig. 2F; Fig. S4). However, both *Q2500≫abi1-1*, which is active in pericycle, endodermis and weakly in cortex, and the ground tissue-specific *J0571≫abi1-1* line displayed discontinuous xylem and double protoxylem, similar to *abi1-1* mutants, whereas the stele-specific *Q0990≫abi1-1* line did not affect xylem development (Fig. 2B-D,F,I). Intriguingly, the epidermal/lateral root cap *J0951≫abi1-1* line also displayed discontinuous xylem strands and double protoxylem (Fig. 2E,F). Furthermore, two independent homozygous endodermis/QC-specific *pSCARECROW::abi1-1* (*pSCR::abi1-1*) lines (Duan et al., 2013) displayed xylem breaks (Fig. 2G,H), supporting the notion that reducing ABA signalling in the endodermis is sufficient to alter normal xylem development.

To assess whether tissue specific ABA signalling inhibition would influence the effect of ABA treatment, we analysed the response of the cell-type-specific *abi1-1* driver lines to 0.5 µM ABA treatment. Stele-specific ABA signalling reduction by *Q0990≫abi1-1* was not sufficient to affect the formation of double protoxylem resulting from the ABA application (Fig. 2I). In contrast, the ground-tissue driver line *J0571≫abi1-1* displayed significantly reduced sensitivity to the ABA treatment (Fisher's exact test, $P<0.05$) (Fig. 2I). These results suggest that ABA predominantly affects stele vascular patterning non-cell-autonomously.

miR165 constitutes a non-cell-autonomous signal responding to ABA

Because miR165 is a well-known signal emanating from the endodermal cell layer to determine vascular patterning (Carlsbecker

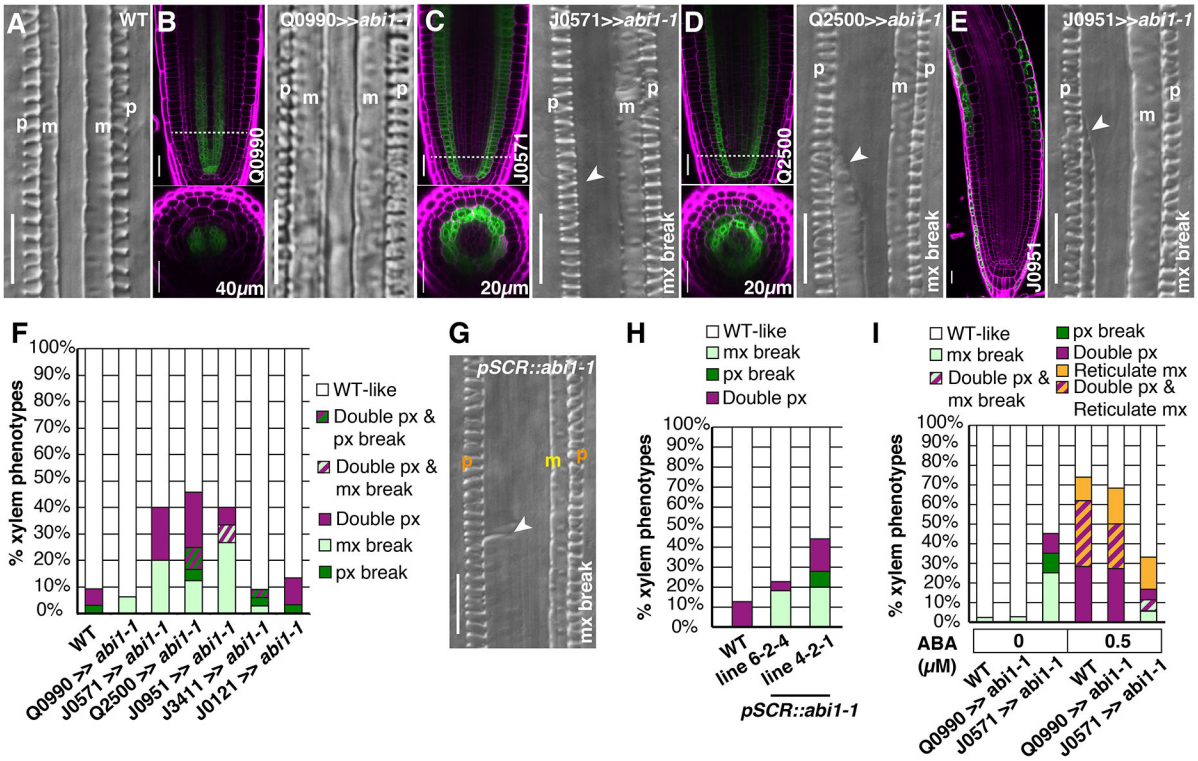

Fig. 2. Non-cell-autonomous control of vascular patterning by ABA signalling. (A) Differential interference contrast (DIC) image of wild-type xylem. (B-E) Confocal images representing the activity domains of GAL4-enhancer trap lines and a DIC image of representative xylem pattern of the respective *abi1-1*-enhancer trap line. Dotted lines indicate position of the optical cross-section. White arrowheads indicate xylem strand breaks. Scale bars: 25 µm for confocal images; 10 µm for DIC images. (F) Quantification of xylem phenotypes of F1 seedlings from crosses between *UAS::abi1-1* and enhancer trap lines (wild type, *n*=32; *Q0990>>abi1-1*, *n*=32; *J0571>>abi1-1*, *n*=30; *Q2500>>abi1-1*, *n*=24; *J0951>>abi1-1*, *n*=30; *J3411>>abi1-1*, *n*=33; *J0121>>abi1-1*, *n*=30). (G) Xylem aberrations in *pSCR::abi1-1*. White arrowhead indicates xylem strand break. Scale bar: 10 µm. (H) Quantification of xylem phenotypes in two independent *pSCR::abi1-1* lines (wild type, *n*=16; *pSCR::abi1-1* line 6-2-4, *n*=22; 4-2-1, *n*=25). (I) Ground tissue and stele-specific *abi1-1* transactivation lines on 0.5 µM ABA (wild type, *n*=42; *Q0990>>abi1-1*, *n*=44; *J0571>>abi1-1*, *n*=18) and mock (wild type, *n*=42; *Q0990>>abi1-1*, *n*=37; *J0571>>abi1-1*, *n*=21). Number of independent experiments performed: F, 4; H, 2; I, 4.

Development (2018) 145, dev159202. doi:10.1242/dev.159202

et al., 2010; Miyashima et al., 2011), we asked whether miR165 could respond to altered ABA levels. Indeed, treatment with 10 µM Flu for 24 h significantly reduced *pMIR165A::GFP* fluorescence intensity (Fig. 3A,B), indicating a requirement of ABA for proper *MIR165A* expression. Similarly, reducing endodermal ABA signalling lowered mature miR165 levels (Fig. 3C) and led to a significant increase in *ATHB8* and *REV* transcript levels (Fig. 3D). Conversely, 4 h treatment with 50 µM ABA resulted in significant upregulation of *pMIR165A::GFP* (Fig. 3E,F), accompanied by a slight but significant increase in mature miR165 levels (Fig. 3G), and significantly reduced *PHB* and *ATHB8* expression levels (Fig. 3H). We have previously shown that a weak miR165-induction line that suppresses *HD-ZIP III* transcript levels to a similar extent is sufficient to cause protoxylem formation in metaxylem position (Müller et al., 2016). Thus, these data suggest that miR165 constitutes a non-cell autonomous endodermis-derived signal affecting xylem development upon alterations in ABA levels.

To further substantiate the involvement of HD-ZIP III TFs in ABA-mediated xylem morphology changes, we took a genetic approach, reasoning that loss-of-function *HD-ZIP III* mutants would display less pronounced phenotypic effects if HD-ZIP III TFs are decisive for the xylem phenotypes under low ABA levels. To test this, we treated *HD-ZIP III* single and double mutants for 72 h with 1 µM Flu. Compared with wild type, all mutants displayed significantly reduced sensitivity to the Flu treatment in terms of frequency of occurrence of discontinuous metaxylem (Fisher's exact test, $P<0.05$) (Fig. S5A). Furthermore, the Flu treatment decreased root length in wild type, but significantly less in *phb-13* (Fig. S6A). Thus, these results suggest that HD-ZIP III TFs are needed for the vascular aberrations inflicted by the Flu treatment. Conversely, if ABA suppresses *HD-ZIP III* expression, we expected an enhanced ABA response in *HD-ZIP III* mutants compared with wild type. We found that although *rev-6* responded similarly to wild type after 72 h of 0.5 µM ABA treatment, all other tested mutants, and particularly *athb8* and *athb8 phb*, were more sensitive to the ABA treatment than wild type (Figs S5A and S6B,C). These results are consistent with our previous findings that mutations in *PHB* and *ATHB8* especially dictate formation of double protoxylem (Carlsbecker et al., 2010). The phenotypic enhancement of the *HD-ZIPIII* single and double mutant xylem phenotypes, which mimic higher order *HD-ZIP III* mutant phenotypes, suggests that ABA negatively affects multiple HD-ZIP III factors.

Taken together, perceived ABA levels affect *MIR165A* activity in the endodermis, leading to alterations in mature miR165 levels and changes in levels of certain HD-ZIP III TFs in the stele, which, at least in part, explains the altered xylem morphology observed under low or high ABA levels or signalling.

Water deficit affects miR165 levels and xylem development

Treatment with exogenous ABA is an often-assumed proxy for abiotic stress, such as limited water availability, which normally rapidly induce elevated endogenous ABA levels (Xiong and Zhu, 2003). However, it is possible that exogenous ABA treatments confer different or non-natural effects. We therefore asked whether limited water availability would cause a similar phenotypic response as application of ABA. To reduce available water under *in vitro* growth, we overlaid agar plates with polyethylene glycol (PEG), following Verslues and Bray (2006), using three different PEG concentrations: 250, 400 and 550 g/l, thereby reducing the water potential to −0.5, −1 and −1.6 MPa, respectively (Fig. S7A). Growth for 72 h on 550 g/l PEG resulted in root growth inhibition in 6-day-old-plants, whereas lower concentrations did not (Fig. 4A). All three PEG concentrations caused double protoxylem and reticulate metaxylem, similar to treatments with ABA (Fig. 4B,C). After 24 h of growth on 550 g/l PEG, 23% displayed double protoxylem or reticulate metaxylem; after 48 h, 53% displayed these phenotypes (Fig. S7B). In line with the double protoxylem formation, *pAHP6::GFP* expanded in 9/22 plants after 12 h

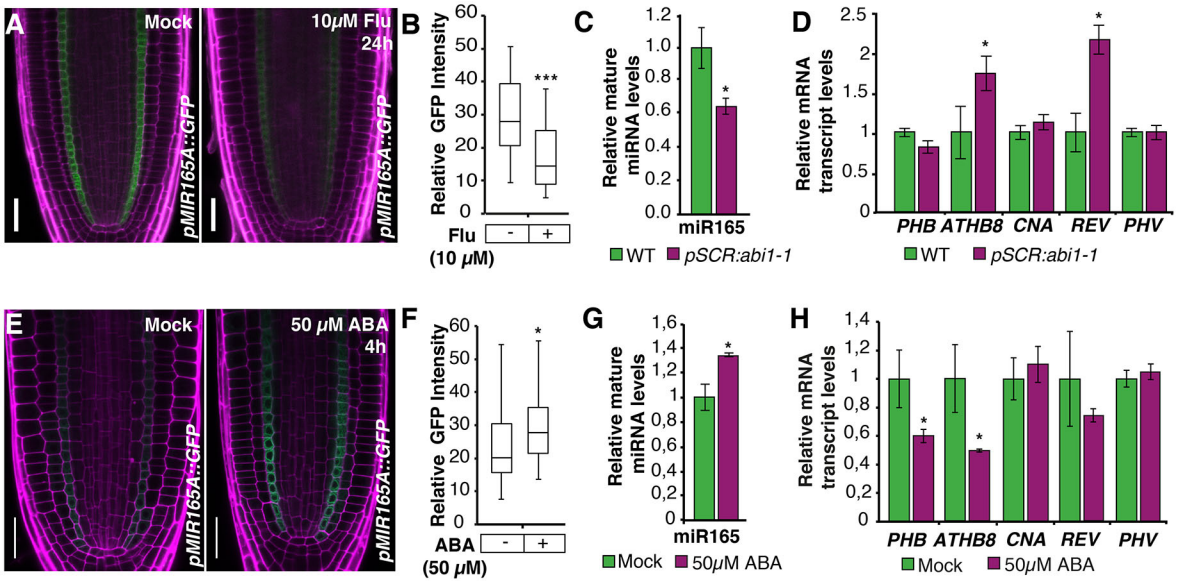

Fig. 3. miR165 levels are affected by ABA. (A) *pMIR165A::GFP* after 24 h treatment of 10 µM Flu compared with mock. (B) Box plot representing background-normalized GFP intensities of *pMIR165A::GFP* upon 10 µM Flu treatment ($n=15$) versus mock ($n=15$). (C,D) qRT-PCR of mature miR165 (C) and HD-ZIP III transcript levels in *pSCR::abi1-1* (D). (E) *pMIR165A::GFP* after 4 h of 50 µM ABA treatment compared with mock. (F) Box plot representing background-normalized GFP intensities of *pMIR165A::GFP* upon 50 µM ABA treatment ($n=26$) versus mock ($n=21$). Intensity settings were kept identical within experiments but may vary between experiments. Scale bars: 25 µm in A and E. (B,F) Bottom and top of the boxes indicate 25th and 75th percentile, respectively. Whiskers extend to minimum and maximum intensity values. *$P<0.05$, ***$P<0.0001$, Mann–Whitney *U*-test. (G,H) qRT-PCR of mature miR165 (G) and *HD-ZIP III* transcript (H) levels in whole roots after 4 h 50 µM ABA. *$P<0.05$, Student's *t*-test, two tailed. Data are mean±s.e.m for C,D,G,H.

Development (2018) 145, dev159202. doi:10.1242/dev.159202

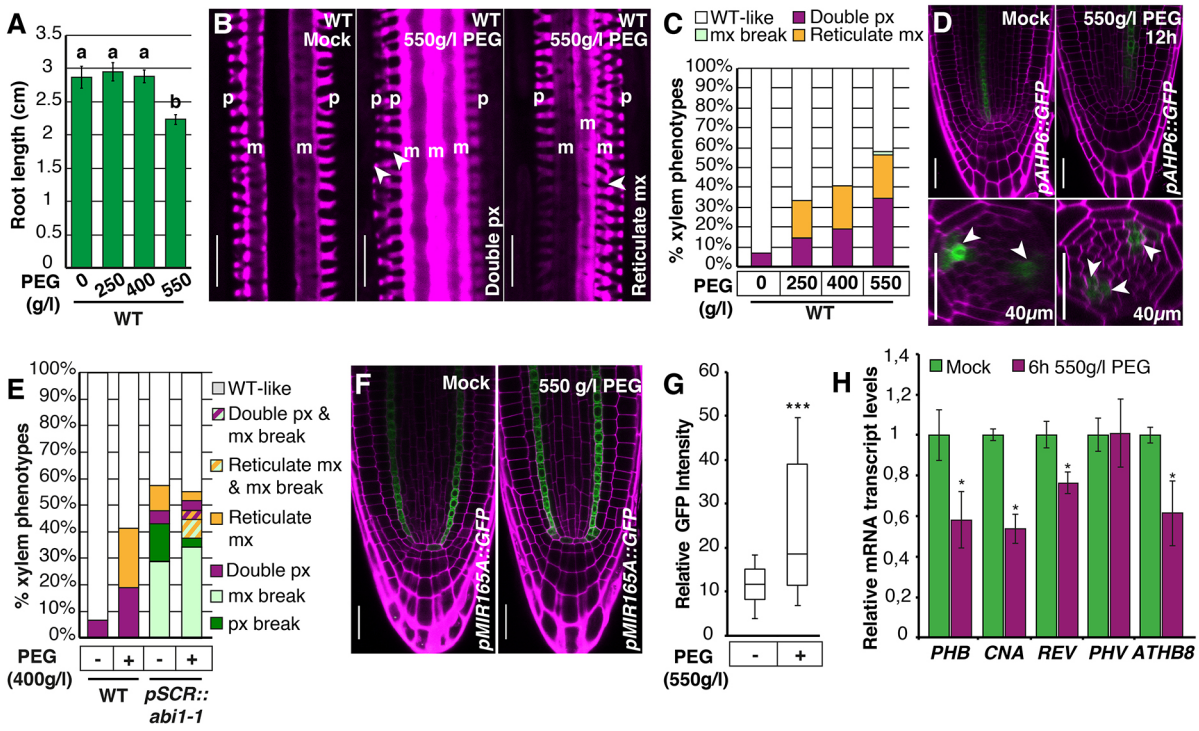

Fig. 4. Xylem morphology is altered upon water-limiting conditions in an ABA- and HD-ZIP III-dependent manner. (A) Root lengths of wild type grown on PEG. a and b indicate groups with significant differences by Tukey's pairwise comparison (n=80). (B) Basic fuchsin-stained wild-type roots grown on PEG. White arrowheads indicate xylem defects. Scale bars: 10 µm. (C) Quantification of xylem phenotypes after 72 h growth on PEG (mock, n=30; 250 g/l PEG, n=48; 400 g/l PEG, n=59; 550 g/l PEG, n=55). (D) *pAHP6::GFP* following 12 h growth on 550 g/l PEG (n=22) and mock (n=12). White arrowheads indicate protoxylem precursor cells. Scale bars: 40 µm. (E) Response of *pSCR::abi1-1* to 72 h growth on 400 g/l PEG (wild-type mock, n=30; wild-type PEG, n=58; *pSCR::abi1-1* mock, n=21; *pSCR::abi1-1* PEG, n=29). (F) *pMIR165A::GFP* after 6 h of 550 g/l PEG treatment. Scale bars: 50 µm. (G) Box plot representing background-normalized GFP intensities of *pMIR165A::GFP* grown under mock conditions (n=19) or on 550 g/l PEG (n=16). Bottom and top of the boxes indicate 25th and 75th percentile, respectively. Whiskers extend to minimum and maximum intensity values. ***P<0.0001, Mann–Whitney U-test. (H) qRT-PCR of *HD-ZIP III* transcript levels after 6 h growth on 550 g/l. Data are mean±s.e.m. in A,H.

growth on 550 g/l PEG (Fig. 4D). Similarly, the number of *pTMO5::n3GFP*-expressing cells increased to six after 48 h of growth on 550 g/l PEG (10/23, 43%) compared with mock, which had five GFP-expressing cells (17/17, 100%) (Fig. S7C). Thus, these results suggest that reduced water availability affects xylem cell identity similarly to exogenous ABA treatment.

The similarities in phenotypes between plants exposed to ABA and low water availability prompted us to investigate whether similar molecular signalling was involved. Reducing ABA signalling using *pSCR: :abi1-1* was sufficient to suppress the xylem phenotype effects of growth on 400 g/l PEG (Fisher's exact text, P<0.05) (Fig. 4E), indicating that endodermal ABA signalling is similarly required for the response to water limitations as for the response to ABA. Furthermore, growth on 550 g/l PEG resulted in a significant upregulation of *pMIR165A::GFP* after 6-8 h (Fig. 4F,G), whereas the mRNA levels of *PHB, CNA*, *ATHB8* and *REV* were reduced after 6 h treatment (Fig. 4H). Moreover, the effects of growth on 250 g/l PEG were greatly enhanced in *phb* such that 61% of the *phb* seedlings displayed double protoxylem compared with 25% for wild type (Fig. S7D). Thus, as summarized in the model in Fig. S8, these results suggest that water deficit invokes alterations in xylem morphology mediated by an ABA-transmitted signal in the endodermis that enhances the levels of miR165, which in turn negatively affects HD-ZIP III TF levels within the stele; this results in changes in xylem development.

Plant survival hinges on adequate responses towards adverse conditions. Here, we show that exposure to water-limiting conditions causes major changes to the root xylem morphology. Similar changes have also been observed in stems of poplar, where water limitation resulted in a decrease in vessel diameter, an increase in vessel number and increase in vessel wall thickness, providing an increased tolerance to cavitation and thereby conferring resistance to water deficit (Awad et al., 2010; Arend and Fromm, 2007). Similarly, soybean plants under water stress increase the number of metaxylem strands, thereby enhancing root hydraulic conductivity (Prince et al., 2017). Upon ABA and PEG treatments, we found that, apart from the formation of extra protoxylem, the metaxylem SCW pattern shifted from pitted to reticulate. A recent study investigated the anatomical characteristics of maize leaf xylem cells upon dehydration and concluded that embolisms formed at a higher rate in metaxylem compared with protoxylem, correlating with the highly hydrophobic SCW pattern of metaxylem cells (Ryu et al., 2016). It will be interesting to test whether the vascular alterations in the *Arabidopsis* root grown under water deficit conditions similarly facilitate water transport.

Cell-type-specific transcriptomic changes have previously been observed in response to various stresses (Dinneny et al., 2008; Geng et al., 2013; Iyer-Pascuzzi et al., 2011). In this study, we found that reducing ABA signalling either in the ground tissue or the epidermis affects stele cell morphology. As the endodermis is the predominant localization for ABA (Ondzighi-Assoume et al., 2016), we focused on signalling mechanisms from endodermis into the stele, but the effects of reduced epidermal ABA signalling indicate the presence of yet another non-cell-autonomous molecular mechanism through

Development (2018) 145, dev159202. doi:10.1242/dev.159202

which ABA affects xylem development. The importance of the endodermis as a signalling hub in mediating stress responses is emphasized by studies showing massive endodermal transcriptome responses and its influence on lateral root formation under salt stress (Duan et al., 2013). The endodermis coordinates cell elongation among tissue layers and undergoes a specific differentiation program, subjected to influences from cues such as nutrient and water availability, to become a barrier between tissues directly exposed to the surrounding environment and those allowing systemic movement of molecules (Doblas et al., 2017; Geldner, 2013). This provides a unique opportunity for the endodermis to act as a signalling centre in the root, within the root meristem, as well as in more differentiated tissues, relaying external stimuli to the interior of the plant. In our study, we contribute with an example of such a signal, miR165, that directly affects the formation of the water-transporting tissue in response to water availability.

MATERIALS AND METHODS

Plant material and growth conditions

Seeds were surface sterilized using chlorine gas for 1-2 h or in 15% bleach solution, imbibed and stratified for 48 h at 4°C, and plated on square plates containing 0.5×MS with 1% (w/v) phytagel or 0.5% (w/v) gelrite, and 0.5% sucrose. For treatments, the plants were germinated on media containing sucrose and then transferred to the treatment plates without sucrose. For experiments in which plants had to be transferred or for collection of roots for expression analysis, seedlings were grown on 25 µm pore Sefar Nitex 03-25/19 mesh as previously described (Müller et al., 2016). The plates were placed vertically in a Sanyo MLR growth cabinet at 22°C and 18 h light and 6 h darkness. For ABA (Sigma) and fluridone (Sigma) treatments, stock solutions of 50 mM and 10 mM in 95% ethanol were used to make media supplemented with different ABA and Flu concentrations. For simulating water-limiting conditions the PEG-overlay method was used (Verslues and Bray, 2006). Briefly, 40 ml of medium without sucrose was poured and allowed to solidify. The solid medium was overlaid with liquid 0.5×MS containing different concentrations (250, 400 or 550 g/l) of PEG 8000 (Sigma). The plates were left overnight and excess PEG solution was then discarded before transfer of plants to the plates. Water activity of the different PEG overlay media was measured using Aqualab Pre Water Activity Meter and results were used to calculate the water potential.

For phenotypic and expression analysis, plants were analysed 5 days after germination, unless otherwise specified. Mutants used in this study include *aba2-1* and *aba3-1* (Léon-Kloosterziel et al., 1996), *abi1-1C* (Kanno et al., 2012), two lines of *pSCR::abi1-1* (Duan et al., 2013), *UAS::abi1-1* (Duan et al., 2013) in Col-0, *abi1-1* and *rev-6* in L*er* (Leung et al., 1994), and *phb-13*, *athb8-11*, *cna-2*, *phb-13 phv-11*, *cna-2 phb-13*, *cna-2 phv-11*, *athb8-11 phb-13*, *athb8-11 phv-11* and *athb8-11 cna-2* (Prigge et al., 2005) in Col *er2*. For tissue-specific expression of *abi1-1*, *UAS::abi1-1* plants were crossed to Haselhoff driver lines (Haseloff, 1999) and F1 plants were analysed. Reporter lines used were *pAHP6*::GFP (Mähönen et al., 2006), *pTMO5::n3GFP* (De Rybel et al., 2013), *pVND7:NLS:YFP* (Kubo et al., 2005) and *pMIR165A::GFP* (Carlsbecker et al., 2010).

Phenotypic analysis

For analysis of primary root xylem defects, seedlings were mounted in 8:2:1 chloral hydrate: glycerol: water (w/v/v) solution and the cleared roots were visualized using a Zeiss Axioscope A1 microscope at 40× magnification, with differential interference contrast (DIC) optics using an Axio Cam ICc5 camera. Each experiment was repeated at least twice. Phenotype quantification was carried out by assessing the vascular defects in each root and representing the frequency of a certain defect in a population. If roots exhibited more than one type of vascular defect, it was quantified in a separate category as individuals exhibiting a combination of phenotypes.

Confocal analysis

Basic fuchsin staining for lignin was performed according to Mähönen et al. (2000), and confocal imaging was carried out using Zeiss 780 inverted Axio Observer with supersensitive GaAsP detector. The brightness and contrast of fuchsin-stained longitudinal and transverse section images were modified using Photoshop (Adobe) for representation of xylem defects. For analysis of GFP-reporter lines, roots were mounted between two coverslips in 40 µM propidium iodide solution and imaged immediately. Confocal analysis was carried out using either a Zeiss LSM 780 or a Zeiss LSM 800 microscope. In each experiment, image acquisition settings were kept constant for mock and respective treatments, and images were acquired at the depth of the QC cells. For quantification of GFP fluorescence intensity, the histogram function in ZEN Black edition software (Zeiss) was used. For *pMIR165A::GFP* quantification, a rectangular area of fixed size was drawn around endodermal cells 9-15, counted from QC, in every root meristem. Another equally sized rectangle was drawn in a region not expressing GFP and used to calculate the background. Background intensities were subtracted from GFP intensities and intensity values were represented in a box plot diagram.

RNA analysis by quantitative RT-PCR

For mRNA transcript quantification analysis, whole roots were collected. For each experiment, three biological replicates consisting of ∼125 individuals each were harvested in RLT buffer from Qiagen Plant Mini Kit and homogenized using Fast prep homogenizer (Savant) at speed 6 for 20 s. RNA extraction and on-column DNase digestion was performed according to the manufacturer's instruction. cDNA was synthesized using iScript cDNA synthesis kit using 500 or 1000 ng of RNA (quantified using Qubit Fluorometer 2.0). For qRT-PCR, iQ SYBR Green Supermix was used in 20 µl reactions and reactions were run in an iCycler iQ Real-Time PCR (Bio-Rad) instrument. Three-step PCR reactions with three technical replicates were carried out with an annealing temperature of 60°C. Results were normalized following the method of Pfaffl (2001) to the reference gene *ADENINE PHOSPHORIBOSYL TRANSFERASE 1* (*APT1*), which was found to be stable and unaffected by ABA treatments (data not shown).

For quantification of mature miRNA levels, whole roots from three biological replicates were collected in 450 µl lysis/binding buffer from the miRvana miRNA Isolation kit (Ambion). Homogenization was carried out as mentioned above and RNA extraction according to manufacturers' instructions. cDNA synthesis was performed using Superscript IV Reverse Transcriptase (Invitrogen) following the stem-loop pulsed reverse transcription protocol (Varkonyi-Gasic et al., 2007). For the reverse transcription of mature miRNA and reference gene, stem loop primers specific for miR165 and primers for *GAPDH* (GAPDH qR) were used in the same reaction (see Table S1). For qRT-PCR, SYBR Green Supermix (Bio-Rad) was used and reactions were performed using the published conditions (Varkonyi-Gasic et al., 2007).

Acknowledgements

We thank A. Minina for technical advice, J. R. Dinneny, T. Hirayama, M. Prigge, A.-P. Mähönen, K. Ohashi-Ito, B. de Rybel and Nottingham Arabidopsis Stock Centre for seeds.

Competing interests

The authors declare no competing or financial interests.

Author contributions

Conceptualization: P.R., G.W., J.d.V., A.C.; Investigation: P.R., G.W., F.A., J.d.V.; Writing - original draft: P.R.; Writing - review & editing: P.R., A.C.; Visualization: P.R.; Supervision: A.C.; Project administration: A.C.; Funding acquisition: A.C.

Funding

Faculty funding to A.C., obtained in a competition, supported the study.

Supplementary information

Supplementary information available online at
http://dev.biologists.org/lookup/doi/10.1242/dev.159202.supplemental

References

Arend, M. and Fromm, J. (2007). Seasonal change in the drought response of wood cell development in poplar. *Tree Physiol.* **27**, 985-992.

Awad, H., Barigah, T., Badel, E., Cochard, H. and Herbette, S. (2010). Poplar vulnerability to xylem cavitation acclimates to drier soil conditions. *Physiol. Plant* **139**, 280-288.

Bartels, P. G. and Watson, C. W. (1978). Inhibition of carotenoid synthesis by Fluridone and Norflurazon. *Weed Sci.* **26**, 198-203.
Carlsbecker, A., Lee, J.-Y., Roberts, C. J., Dettmer, J., Lehesranta, S., Zhou, J., Lindgren, O., Moreno-Risueno, M. A., Vatén, A., Thitamadee, S. et al. (2010). Cell signalling by microRNA165/6 directs gene dose-dependent root cell fate. *Nature* **465**, 316-321.
Cutler, S. R., Rodríguez, P. L., Finkelstein, R. R. and Abrams, S. R. (2010). Abscisic acid: emergence of a core signaling network. *Annu. Rev. Plant Biol.* **61**, 651-679.
De Rybel, B., Möller, B., Yoshida, S., Grabowicz, I., Barbier de Reuille, P., Boeren, S., Smith, R. S., Borst, J. W. and Weijers, D. (2013). A bHLH complex controls embryonic vascular tissue establishment and indeterminate growth in Arabidopsis. *Dev. Cell* **24**, 426-437.
Dinneny, J. R., Long, T. A., Wang, J. Y., Jung, J. W., Mace, D., Pointer, S., Barron, C., Brady, S. M., Schiefelbein, J. and Benfey, P. N. (2008). Cell identity mediates the response of Arabidopsis roots to abiotic stress. *Science* **320**, 942-945.
Doblas, V. G., Geldner, N. and Barberon, M. (2017). The endodermis, a tightly controlled barrier for nutrients. *Curr. Opin. Plant Biol.* **39**, 136-143.
Duan, L., Dietrich, D., Ng, C. H., Chan, P. M. Y., Bhalerao, R., Bennett, M. J. and Dinneny, J. R. (2013). Endodermal ABA signaling promotes lateral root quiescence during salt stress in Arabidopsis seedlings. *Plant Cell* **25**, 324-341.
Eldem, V., Çelikkol Akçay, U., Ozhuner, E., Bakır, Y., Uranbey, S. and Unver, T. (2012). Genome-wide identification of miRNAs responsive to drought in peach (*Prunus persica*) by high-throughput deep sequencing. *PLoS ONE* **7**, e50298.
Geldner, N. (2013). The endodermis. *Annu. Rev. Plant Biol.* **64**, 531-558.
Geng, Y., Wu, R., Wee, C. W., Xie, F., Wei, X., Chan, P. M. Y., Tham, C., Duan, L. and Dinneny, J. R. (2013). A spatio-temporal understanding of growth regulation during the salt stress response in Arabidopsis. *Plant Cell* **25**, 2132-2154.
Ghassemian, M., Nambara, E., Cutler, S., Kawaide, H., Kamiya, Y. and McCourt, P. (2000). Regulation of abscisic acid signaling by the ethylene response pathway in Arabidopsis. *Plant Cell* **12**, 1117-1126.
Giusti, L., Mica, E., Bertolini, E., De Leonardis, A. M., Faccioli, P., Cattivelli, L. and Crosatti, C. (2017). microRNAs differentially modulated in response to heat and drought stress in durum wheat cultivars with contrasting water use efficiency. *Funct. Integr. Genomics* **17**, 293-309.
Haseloff, J. (1999). GFP variants for multispectral imaging of living cells. *Methods Cell Biol.* **58**, 139-151.
Iyer-Pascuzzi, A. S., Jackson, T., Cui, H., Petricka, J. J., Busch, W., Tsukagoshi, H. and Benfey, P. N. (2011). Cell identity regulators link development and stress responses in the Arabidopsis root. *Dev. Cell* **21**, 770-782.
Kanno, Y., Hanada, A., Chiba, Y., Ichikawa, T., Nakazawa, M., Matsui, M., Koshiba, T., Kamiya, Y. and Seo, M. (2012). Identification of an abscisic acid transporter by functional screening using the receptor complex as a sensor. *Proc. Natl. Acad. Sci. USA* **109**, 9653-9658.
Kantar, M., Unver, T. and Budak, H. (2010). Regulation of barley miRNAs upon dehydration stress correlated with target gene expression. *Funct. Integr. Genomics* **10**, 493-507.
Kubo, M., Udagawa, M., Nishikubo, N., Horiguchi, G., Yamaguchi, M., Ito, J., Mimura, T., Fukuda, H. and Demura, T. (2005). Transcription switches for protoxylem and metaxylem vessel formation. *Genes Dev.* **19**, 1855-1860.
Léon-Kloosterziel, K. M., Gil, M. A., Ruijs, G. J., Jacobsen, S. E., Olszewski, N. E., Schwartz, S. H., Zeevaart, J. A. D. and Koornneef, M. (1996). Isolation and characterization of abscisic acid-deficient Arabidopsis mutants at two new loci. *Plant J.* **10**, 655-661.
Leung, J., Bouvier-Durand, M., Morris, P. C., Guerrier, D., Chefdor, F. and Giraudat, J. (1994). Arabidopsis ABA response gene ABI1: features of a calcium-modulated protein phosphatase. *Science* **264**, 1448-1452.
Mähönen, A. P., Bonke, M., Kauppinen, L., Riikonen, M., Benfey, P. N. and Helariutta, Y. (2000). A novel two-component hybrid molecule regulates vascular morphogenesis of the Arabidopsis root. *Genes Dev.* **14**, 2938-2943.
Mähönen, A. P., Bishopp, A., Higuchi, M., Nieminen, K. M., Kinoshita, K., Törmäkangas, K., Ikeda, Y., Oka, A., Kakimoto, T. and Helariutta, Y. (2006). Cytokinin signaling and its inhibitor AHP6 regulate cell fate during vascular development. *Science* **311**, 94-98.
Meyer, K., Leube, M. P. and Grill, E. (1994). A protein phosphatase 2C involved in ABA signal transduction in *Arabidopsis thaliana*. *Science* **264**, 1452-1455.
Miyashima, S., Koi, S., Hashimoto, T. and Nakajima, K. (2011). Non-cell-autonomous microRNA165 acts in a dose-dependent manner to regulate multiple differentiation status in the Arabidopsis root. *Development* **138**, 2303-2313.
Müller, C. J., Valdés, A. E., WANG, G., Ramachandran, P., Beste, L., Uddenberg, D. and Carlsbecker, A. (2016). PHABULOSA mediates an auxin signaling loop to regulate vascular patterning in Arabidopsis. *Plant Physiol.* **170**, 956-970.
Ondzighi-Assoume, C. A., Chakraborty, S. and Harris, J. M. (2016). Environmental nitrate stimulates abscisic acid accumulation in Arabidopsis root tips by releasing it from inactive stores. *Plant Cell* **28**, 729-745.
Osakabe, Y., Osakabe, K., Shinozaki, K. and Tran, L.-S. P. (2014). Response of plants to water stress. *Front. Plant Sci.* **5**, 86.
Pfaffl, M. W. (2001). A new mathematical model for relative quantification in real-time RT-PCR. *Nucleic Acids Res.* **29**, e45.
Prigge, M. J., Otsuga, D., Alonso, J. M., Ecker, J. R., Drews, G. N. and Clark, S. E. (2005). Class III homeodomain-leucine zipper gene family members have overlapping, antagonistic, and distinct roles in Arabidopsis development. *Plant Cell* **17**, 61-76.
Prince, S. J., Murphy, M., Mutava, R. N., Durnell, L. A., Valliyodan, B., Shannon, J. G. and Nguyen, H. T. (2017). Root xylem plasticity to improve water use and yield in water-stressed soybean. *J. Exp. Bot.* **68**, 2027-2036.
Reinhart, B. J., Weinstein, E. G., Rhoades, M. W., Bartel, B. and Bartel, D. P. (2002). MicroRNAs in plants. *Genes Dev.* **16**, 1616-1626.
Rhoades, M. W., Reinhart, B. J., Lim, L. P., Burge, C. B., Bartel, B. and Bartel, D. P. (2002). Prediction of plant microRNA targets. *Cell* **110**, 513-520.
Ryu, J., Hwang, B. G., Kim, Y. X. and Lee, S. J. (2016). Direct observation of local xylem embolisms induced by soil drying in intact *Zea mays* leaves. *J. Exp. Bot.* **67**, 2617-2626.
Varkonyi-Gasic, E., Wu, R., Wood, M., Walton, E. F. and Hellens, R. P. (2007). Protocol: a highly sensitive RT-PCR method for detection and quantification of microRNAs. *Plant Methods* **3**, 12.
Verslues, P. E. and Bray, E. A. (2006). Role of abscisic acid (ABA) and *Arabidopsis thaliana* ABA-insensitive loci in low water potential-induced ABA and proline accumulation. *J. Exp. Bot.* **57**, 201-212.
Xiong, L. and Zhu, J.-K. (2003). Regulation of abscisic acid biosynthesis. *Plant Physiol.* **133**, 29-36.
Zhang, H., Han, W., De Smet, I., Talboys, P., Loya, R., Hassan, A., Rong, H., Jürgens, G., Paul Knox, J. and Wang, M.-H. (2010). ABA promotes quiescence of the quiescent centre and suppresses stem cell differentiation in the Arabidopsis primary root meristem. *Plant J.* **64**, 764-774.